Title

Kinetics of Pore Coarsening in Glassy Carbon

Authors

Bose, S
Bragg, R H

Publication Date

1980-09-01

LBL-7659 Rev.
Preprint

Lawrence Berkeley Laboratory
UNIVERSITY OF CALIFORNIA

Materials & Molecular Research Division

Published in Carbon

KINETICS OF PORE COARSENING IN GLASSY CARBON

S. Bose and R.H. Bragg

September 1980

Prepared for the U.S. Department of Energy under Contract W-7405-ENG-48

DISCLAIMER

KINETICS OF PORE COARSENING IN GLASSY CARBON

S. Bose* and R. H. Bragg

Department of Materials Science and Mineral Engineering
and Materials and Molecular Research Division
of Lawrence Berkeley Laboratory, University of California, Berkeley, CA

Abstract

One third of the microstructure of glassy carbon (GC) consists of closed pores. Density measurements indicate that the total pore volume depends only on the heat treatment temperature and not on the heat treatment time, a characteristic of coarsening. The kinetics of coarsening of these pores on heat treatment has been investigated by analyzing the changes in specific surface area of the pores as determined by the small angle x-ray scattering (SAXS) technique. A part of the surface area change is due to thermal expansion induced microcracking. Both the superposition method after correcting the thermal expansion induced surface area change and the curve fitting method give an activation energy of 64 ±10 kcal/mole. This value is compared with the activation energies of various rate processes in graphite. A model of coarsening of the pores based on a vacancy migration mechanism is proposed.

This work was supported by the Director, Office of Energy Research, Office of Basic Energy Sciences, Materials Science Division of the U.S. Department of Energy under Contract No. W-7405-ENG-48.

---

*Present address: United Technologies, Power System Division, P.O. Box 109, South Windsor, Connecticut 06074.

1. INTRODUCTION

Production of disordered carbons by the pyrolysis and heat treatment of thermosetting polymers above 1000°C is an area of technological interest. The residue of the process is termed glassy carbon (GC). The microstructure of GC contains a significant volume of micropores as indicated by its low density (1.5 gm/cm^3 compared to 2.27 gm/cm^3 for single crystal graphite) while the crystallographic parameters c and a are not significantly different from those of graphite. Using small angle x-ray scattering (SAXS) Rothwell[1] showed that the pores are in the size range of a few Å. The size and shapes of these pores were also characterized by Perret and Ruland[2] using SAXS. The specific surface area of the pores, as measured by these authors, is of the order of several hundred m^2/cm^3. The small size of the pores had obviously been a deterrent in their visual observation. The specific surface area of the pores has been known to decrease[2] with increased heat treatment. In the present investigation an effort has been made to monitor changes in the pores affected by the heat treatment and to understand the kinetics of the process involved. The material used for the study has been well characterized using x-ray diffraction (XRD) and transmission electron microscopy (TEM). Bulk density measurements were used as a first step in determining the pore volumes. Small angle x-ray scattering has been used to follow the kinetics of surface area change on heat treatment.

2. MATERIAL AND HEAT TREATMENT

The GC used in the present study was made by Polycarbon, Inc., North Hollywood, CA. The materials received from the manufacturer were in the form of plates 20.3 x 5.1 x 0.16 cm heat treated at 1000°C for 1 hour. Using a diamond saw, small pieces 5.1 x 2.5 x 0.16 cm were cut from the plates and

subsequently heat treated at selected temperatures (HTT) for various lengths of time (HTt). Part of the heat treatment was done in a Pereny furnace and the remainder in an Astro furnace. A Leeds and Northrup optical pyrometer calibrated in the temperature range 1000°C - 3000°C was used to measure temperature. Above 2000°C the precision of temperature measurement was ±20°C. Heat treatment was done in pure argon or Helium atmosphere with a heating rate between 70°C/min and 100°C/min.

3. MICROSTRUCTURE

Unlike that of crystalline materials, the XRD line profile of GC is characterized by a few broad and diffuse peaks at the approximate positions of the (002), (100), (004), and (110) reflections of graphite, superimposed on a high background, and a strong small angle intensity. After appropriate corrections[3] the true interference function is obtained. In the absence of higher order peaks removal of strain broadening is not feasible. The "apparent" crystallite sizes determined from the corrected XRD line profiles are found to increase relatively slowly[4] with increasing HTT. L_a increases from 22Å to 50Å, while L_c increases from 10Å to 28Å in the HTT range 1000-2700°C, HTt being 2 hours. There is a plateau in the layer separation with d_{002} approximately constant at 3.44Å in the HTT range of 1000°C - 2300°C beyond which it decreases again but never goes below 3.40Å indicating the characteristic turbostratic nature of GC.

A high resolution transmission electron microscopic lattice image was obtained from a sample prepared by the ion milling technique. The selected area diffraction did not show any spot patterns. The lattice image obtained

by the two beam technique[5] showed the tangled lathlike microstructure in agreement with the observations made by other workers.

4. DENSITY MEASUREMENTS

The density of GC samples heat treated at several temperatures for various lengths of time was measured using room temperature water as pycnometer fluid since previous workers have shown that within the limits of experimental error the helium density of GC was identical with the water density. The variation in density of GC was recorded at each temperature as a function of HTt and also as a function of HTT keeping the samples for up to 10 hrs at each temperature.

5. SMALL ANGLE X-RAY SCATTERING (SAXS)

Theory: The SAXS technique was successfully applied by Guinier to study the kinetics of GP zone formation in age hardening alloys. Later this technique was used by Rothwell[1] and Perret and Ruland[2] to investigate some aspects of pores in GC. The theory of SAXS[6] for centrosymmetric electron density $\rho(\bar{u})$ gives the intensity scattered with a wave vector $\bar{h}$ ($|h| = 4\pi\sin\theta/\lambda$; 2θ = angle of scattering).

$$I(h) = V\langle\rho^2\rangle \int_0^\infty 4\pi r^2 C(r) \sin hr/hr \, dr \qquad (1)$$

where the Debye correlation function C(r) is given by

$$C(r) = \int_V \rho(\bar{u})\rho(\bar{u} + \bar{r})/V\langle\rho^2\rangle \, dV_{\bar{u}} .$$

Some limiting cases of equation (1) are:

$h \to o$ (Guinier region; small angles in SAXS)

$$I(h) = V\langle\rho^2\rangle \exp(-1/3\ h^2Rg^2) \qquad (2)$$

where Rg is the electron radius of gyration, sometimes called the 'Guinier radius'. For an infinitely long and narrow slit collimator Eqn. (2) remains intact except for a constant factor dependent on Rg.

$h \to \infty$ (Porod region; large angles in SAXS)

$$I(h) = 2\pi\langle\rho^2\rangle\ S/h^4$$

where S is the interface area of the two phase scattering system. For infinitely long and narrow slits this equation reduces to

$$I(h) = \pi^2\langle\rho^2\rangle\ S/h^3 \qquad (3)$$

The integrated intensity for slit systems is given by

$$\int_0^\infty I(h)\ hdh = 4\pi^2\langle\rho^2\rangle V\ c(1-c)$$

where c is the volume fraction of one phase and V is the total irradiated volume. The specific surface area is therefore given by

$$S/V = 4c(1-c)\ \text{Lim}\ h^3I(h) \Big/ \int_0^\infty hI(h)dh \qquad (4)$$

Equation (4) is of general validity even for dense systems where inter-particle interference is present.

Porod[7] showed that for smooth interfaces between two phases in a scattering system a plot of $h^3\ I(h)$ vs h will have a maximum while no maximum

will be observed if the interface has sharp edges and corners. These predictions have been verified experimentally by Tchoubar and Mering[8].

To use Eqn. (4) in the determination of specific surface area one needs to know the integral in the denominator. The limit of integration extends from $h = 0$ to $h \to \infty$, but $I(h)$ can only be recorded within a limited range of h. For $h \sim o$, $hI(h)$ is very small irrespective of the accuracy of $I(h)$. However, for large h there is considerable chance of error in $I(h)$ because it becomes small. This error is avoided to some extent by splitting the integral to take advantage of Porod's Law.

$$\int_o^\infty hI(h)dh = \int_o^{h_o} hI(h)dh + \int_{h_o}^\infty h\, k/h^3 dh$$

$$= \int_o^{h_o} hI(h)dh + \frac{k}{h_o}$$

where k is the limiting value of $h^3I(h)$ obtained from a plot of $h^3I(h)$ vs h or h^2. h_o has to be within the range where Porod's Law holds.

Experiment: SAXS data were recorded using a GE XRD-3 diffractometer with a modified slit arrangement such that the infinite slit geometry condition[1] was found to be satisfied. CuK_α radiation was used in conjunction with a Ni filter and a pulse height analyzer. The detector was a scintillation counter. Data were recorded on a chart for 2θ angles between 0.4° and 7°. GC samples in the form of $1/\mu$ thick plates were placed in transmission geometry, μ being the linear absorption coefficient. Background corrections were made.

6. RESULTS

The density of GC as a function of HTt is shown in Fig. 1 where each set of data corresponds to the indicated HTT. It is clear that the density remains constant, independent of HTt as long as HTT is kept constant. In other words the total pore volume remains constant, independent of HTt as long as HTT is constant. The isochronal variation of the density of GC with HTT is shown in Fig. 2, HTt being 10 hrs. at each temperature. It is evident that density decreases by as much as 13% giving an unusual material that becomes more porous on heat treatment at higher temperatures. Fischbach and Rorabaugh[9] have also observed a similar trend in density variation with heat treatment.

Fig. 3 shows a typical intensity distribution of SAXS where intensity I is plotted against absolute value of wave vector h on a log-log scale. The distribution is similar to those obtained by Rothwell[1] and Peret and Ruland[2] except that in the region of large h a slope of -3 is achieved. The rise in intensity at small angles ($h\ 2<10^{-2}\text{Å}^{-1}$) is known to be a composite effect of multiple scattering and double diffraction from the layer type planes of GC. The radius of gyration Rg of pores[6] was determined from the slope of the Guinier plots shown in Fig. 4 where Log I is plotted against h^2. As expected from Eqn. (2) a set of straight lines is obtained. The radius of gyration so determined is weighted towards larger pores because it is the larger pore that contribute more intensity in the Guinier region. Radius of gyration kinetics is shown in Fig. 5. While it is clear that rate processes are indeed involved, it was not possible to analyze the Rg kinetics, possibly because of the ambiguous meaning associated with Rg when pore shapes are not simple.

A more fundamental quantity which is relatively independent of the size distribution and the model of the pore geometry is the specific surface area of the pore-matrix interface. The specific surface area has been determined using Eqn. (4). The limiting value of $h^3I(h)$ was determined by plotting this quantity against h^2 as shown in Fig. 6. The quantity in the denominator of Eqn. (4) was determined by plotting $I(h)$ vs h^2 and measuring the area under the curve (x 0.5) bounded between $h = 0$ and an arbitrary value of h that lies in the horizontal portion of Fig. 6. Figure 7 shows the specific surface area kinetics for HTT ranging from 2000 to 2700°C.

Fischbach's[15] superposition technique to determine the activation energy could not be applied directly to the data of Figure 7 because a part of the surface area change from one HTT to another was found to be thermal expansion induced i.e, non-kinetic. However, it is not necessary to employ the superposition technique if a kinetic analysis of the data can be made. It is reasonable to attempt an analysis in terms of a first order rate law whose differential equation is

$$\frac{d}{dt}(s_t - s_\infty) = -k(T)(S_t - S_\infty)$$

where $k(T)$ is the rate constant and s_t is the specific surface area S/V. The solution is

$$s_t = s_\infty + (s_0 - s_\infty)\exp(-kt)$$

where $k = k(T)$ depends upon HTT through the Arrhenius equation

$$k(T) = k_0 \exp(-\Delta H/RT).$$

In this equation ΔH is the activation energy per mole for the associated process. The hypothesis of a first order rate process can be tested by first analysing the data of Fig. 7 to obtain data of $k(T)$, s_0 and s_∞ for each HTT. Using these parameters graphs of s_t vs $\exp(-kT)$ can be plotted and should be found to be straight lines. Figure 8 shows the results of such an analysis. Figure 9 shows that when the values of $k(T)$ used to obtain Fig. 8 are plotted as $\ell n\ k$ versus $1/T$ a straight line of negative slope is obtained, from which ΔH can be calculated. Thus to a good approximation it appears that the process obeys first order kinetics with a single activation energy. It is not necessary to resort to a superposition analysis.

To conduct a superposition analysis of the data it is necessary to correct for the non-kinetic changes in S/V. The component of the specific surface area change which is due to thermal expansion alone can be estimated from Fig. 8 by noting the relative shifts between the sets of data for each temperature. The thermal expansion induced S/V changes, determined as discussed above have been plotted against the temperature as shown in Fig. 10. This component has been added to the corresponding data relative to 2000°C HTT and replotted in Fig. 11. The corrected surface areas can now be superimposed by relative translation along the time axis, as shown in Fig. 12 where 2700°C HTT has been taken as the reference. The relative shifts thus obtained have also been plotted against $1/T$ in Fig. 9 to determine the activation energy. It can be seen that the data from curve fitting and from superposition agree very well. From the slope of curve Fig. 9 the activation energy of the rate process is found to be 64±10kcal/mole

(2.8±0.4 eV/atom).

7. DISCUSSION

The constancy of total pore volume as long as HTT was kept constant, in conjunction with the fact that the specific surface area of the pores decreases with HTt, indicates that pores are coarsening.

The increase in porosity as HTT increased is probably caused by two mechanisms. One is the swelling due to expansion of pyrolysis gases, the other being the rupture of pore edges due to thermal stresses generated because of anisotropic thermal expansion. The decrease in density with increase in HTT has been known to depend on the rate of heating the sample[13]. This is due to the fact that pyrolysis gases trapped in pores are slow in diffusing out.

For the second mechanism an approximate estimate of the thermal stress acting at pore edges can be calculated. Using $\alpha_c = 26.5 \times 10^{-6}/°C$ and $\alpha_a = 1.2 \times 10^{-6}/°C$, α being the coefficient of thermal expansion, one gets a maximum strain ε of 0.05 at 2000°C. The maximum thermal stress is

$$\sigma \simeq c_{11}\varepsilon$$

where c_{11} is very large compared to the other stiffness components. Using $c_{11} = 106 \times 10^{11}$ dynes/cm^2 one obtains

$$\sigma = 5.4 \times 10^{11} \text{ dynes/cm}^2$$

This stress is of the same order of magnitude as the failure stress of graphite in the presence of 10Å Griffith flaws comparable to the size of the pores discussed. It is therefore likely that rupture of pore edges due to thermal stress is the major contributing factor in increasing the porosity of GC as HTT is increased.

Bragg, Mehrotra and Rao[14] have provided further evidence in favor of an irreversible thermal expansion induced microcracking. They measured changes in mass, volume and pycnometric density in the range 1000°C-2700°C and found that the mass losses never exceeded one percent. The much larger dimensional changes were comparable to those expected if GC suffered irreversible thermal expansion for HTT greater than the 1000°C process temperature. Additional support to the thermal expansion mismatch induced surface area change is seen in Fig. 10 which shows an approximately linear relationship between S/V changes and the temperature of heat treatment as expected on this mechanism.

The activation energy determined for GC pore growth should be compared with those of rate processes in graphite. Table 1 lists some of the activation energies for graphite and graphitizable carbons. Vacancy migration in the layer plane seems to have an activation energy closest to that observed. Because small pores are available which could both be the source and sinks of vacancies, interstitial migration in the c-axis direction having a similar activation energy seems to be a relatively insignificant mechanism. Any model that is accepted as the predominant activated process leading to the reduction in specific surface area of pores in GC should be capable of explaining the following observations:

GC undergoes only limited graphitization.

The total pore volume remains constant as long as HTT is kept constant.

The tangled microstructure has its own constraints and does not allow extensive realignment.

A model that could explain these observations is shown in Fig. 13. a and b are pores with the layer planes making the pore walls. The layer planes of graphite have very small surface energy, about 100 ergs/cm^2[10], compared to that of any other plane. Thus the driving force for the surface area reduction would be very small. Any reduction in the surface area of these types of pores would need a coordinated breaking and making of bonds at the pore surfaces. This seems thermodynamically improbable. Therefore the pores of geometry a and b seem to be stable. Pores c and d, however, are in the layer planes going through the stacks. Their surfaces are mostly of high energy and the surface energy is obviously not constant over the whole surface because of the anisotropy of the graphite structure. A large pore c situated at a bend and a small one d at a relatively straight portion will have two sources of driving force for surface area reduction. One is the reduction in total surface energy and the other is the reduction of strain energy on removing the bent regions of the stack by migration of atoms around c towards the smaller pore d. This is the same as vacancy migration from d towards c, thereby coarsening the larger pore c and shrinking the smaller one d.

No effort is made here to determine the relative importance of strain energy vis-a-vis surface energy of pores. The model put forward would lead to "graphitization" around the micro pores such as d because here layer extensions are occurring at pore site d. While the graphitization at micropores have not been investigated, there is evidence of graphitization around macropores[11,12]. If, however, there are constraints like another stack f blocking the growth of layer planes or if there are no sink pores nearby, graphitization would be halted. Since the pores of type c and d are

outnumbered by those of types a and b, and since there are extensive constraints like f, only limited graphitization occurs. As the total number of vacancies moving out of a pore equals that going into sink pores, the overall pore volume does not change with HTt.

The present mehtod of investigation probes only the regions near the pores and therefore does not detect processes going on in the bulk away from pores. The bulk graphitization which has an activation energy higher than that observed in this investigation, does not, therefore, interfere with the present analysis.

ACKNOWLEDGEMENT

The authors are thankful to Prof. D. B. Fischbach of the University of Washington, Seattle for his comments on the earlier drafts of this paper. This work was supported by the Division of Materials Sciences, U.S. Department of Energy under contract No. W-7405-Eng-48.

REFERENCES

1. W. S. Rothwell, J. Appl. Phys., 39, 1840 (1968).
2. R. Perret and W. Ruland, J. Appl. Cryst., 5, 183 (1972).
3. S. Bose and R. H. Bragg, Lawrence Berkeley Laboratory Report #6649 (1978).
4. R. Saxena and R. H. Bragg, Carbon, 16, 373 (1978).
5. S. Bose, U. Dahmen, R. H. Bragg and G. Thomas, J. Amer. Ceram. Soc., 61, 174 (1978).
6. A. Guinier and G. Fournet, Small Angle X-ray Scattering of X-rays, John Wiley and Sons, Inc., London (1955).
7. G. Porod, Small Angle X-ray Scattering (Ed. H. Brumberger), Gordon and Beach, New York (1967).
8. D. Tchoubar and J. Mering, J. Appl. Cryst., 2, 128 (1969).
9. D. B. Fischbach and M. E. Rorabaugh, Deutsche Keramische Gesellschaft Carbon '76 (1976), p. 185; High Temperature - High Pressure 9, 199 (1977).
10. R. J. Good, L. S. Girifalco and G. J. Kraus, J. Phys. Chem., 62, 1418 (1958).
11. K. Kawamura and T. Tsuzuku, Carbon, 12, 352 (1974).
12. K. Kamiya and K. Suzuki, Carbon, 13, 317 (1975).
13. D. B. Fischbach and M. E. Rorabaugh, 13th Biennial Carbon Conference, Irvine, July 19-7 (Post Deadline Paper).
14. R. H. Bragg, B. Mehrotra and A. S. Rao, Lawrence Berkeley Laboratory Report #10623 (1980).
15. D. B. Fischbach, Jet Propulsion Laboratory Technical Report #32-532 (1966).

FIGURE CAPTIONS

1. Kinetics of density change in GC.
2. Density of GC as a function of heat treatment temperature.
3. Typical Porod plot of SAXS from GC.
4. Typical Guinier plot of SAXS from GC.
5. Radius of gyration kinetics of pores in GC.
6. Plot to determine the Porod invariant in SAXS from GC.
7. Specific surface area kinetics of pores in GC.
8. Specific surface area of pores in GC follows a first order rate law with k as rate constant.
9. Activation energy of pore surface area evolution in GC.
10. Thermal expansion induced surface area change as a function of HTT.
11. Specific surface area kinetics of pores in GC, corrected for thermal expanison induced surface area change.
12. Superimposition of corrected specific surface areas.
13. Pore model in GC.

Table 1.

VARIOUS ACTIVATION ENERGIES FOR GRAPHITE

Mechanism	Energy eV/atom
Vancancy formation	7.0 ± 0.5
Interstitial formation	7.5 ± 1.8
Vacancy migration (a direction)	3.1 ± 0.2
Vancancy migration (c direction)	> 5.5
Interstitial migration (a direction)	< 0.1
Interstitial migration (c direction)	2.8 ± 0.2
Self diffusion	
Synthetic (bulk)	1.7
Synthetic (grist)	2.0
Single crystal	7.2
Synthetic pile grade	3.5 - 6.5
Heat of sublimation	7.43
Graphitization (graphitizable carbon)	11.3

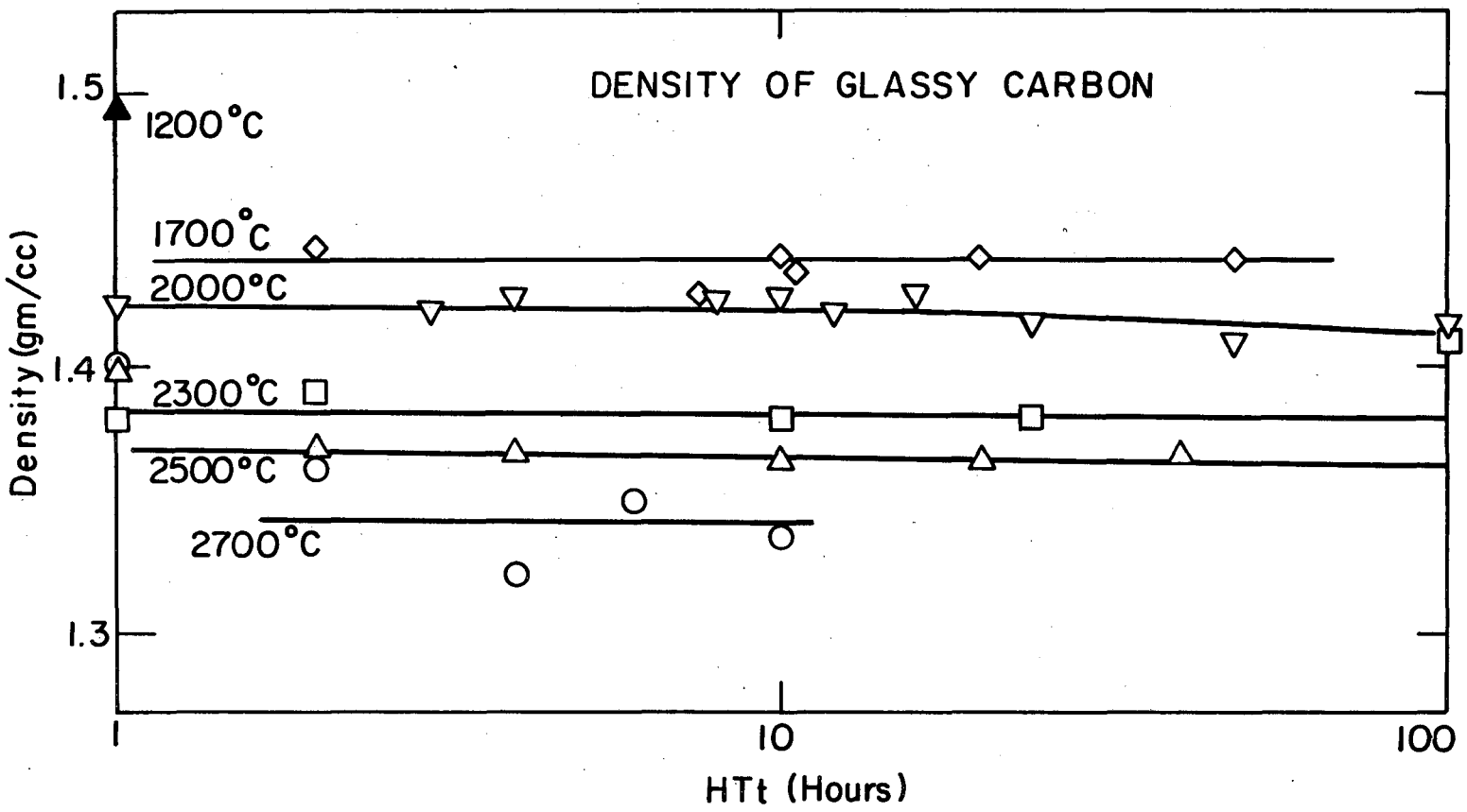
DENSITY OF GLASSY CARBON
1.5
1.4
1.3
1200°C
1700°C
2000°C
2300°C
2500°C
2700°C
Density (gm/cc)
1
10
100
HTt (Hours)
XBL 776-5645

Fig. 1

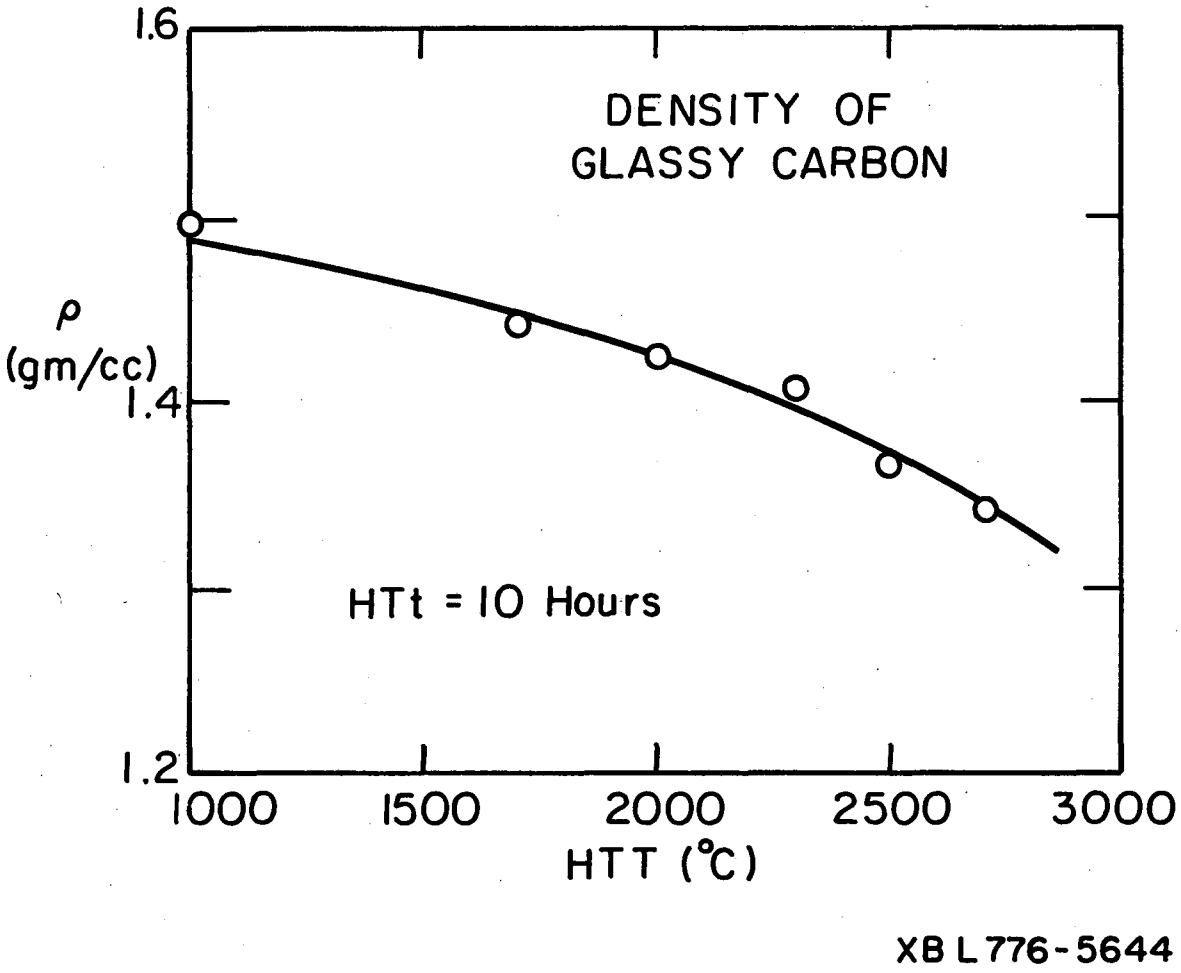
DENSITY OF
GLASSY CARBON
ρ
(gm/cc)
1.6
1.4
1.2
HTt = 10 Hours
1000
1500
2000
2500
3000
HTT (°C)
XBL776-5644

Fig. 2

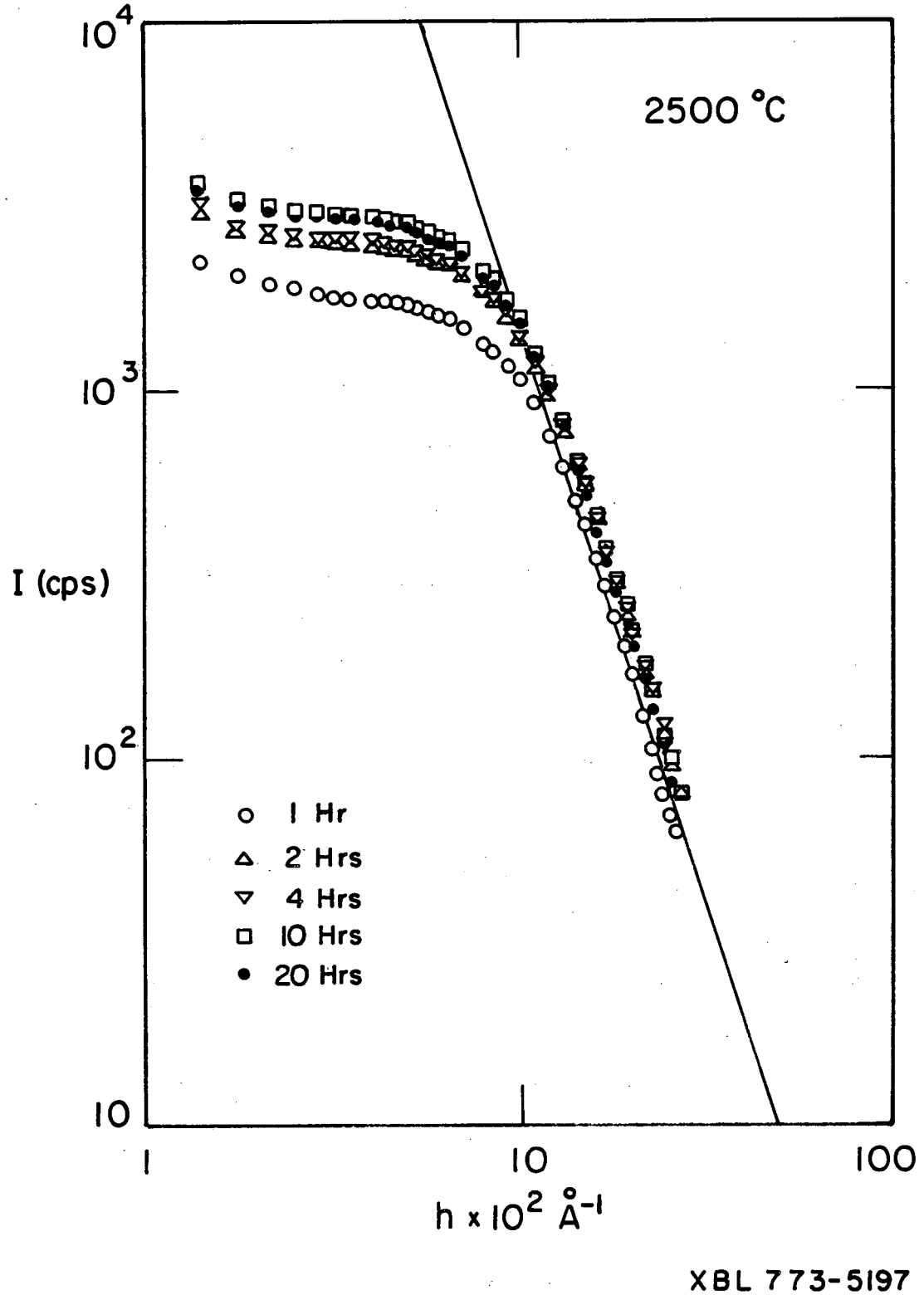
2500 °C
I (cps)
10^4
10^3
10^2
10
1
10
100
h x 10^2 Å^{-1}
1 Hr
2 Hrs
4 Hrs
10 Hrs
20 Hrs
XBL 773-5197

Fig. 3

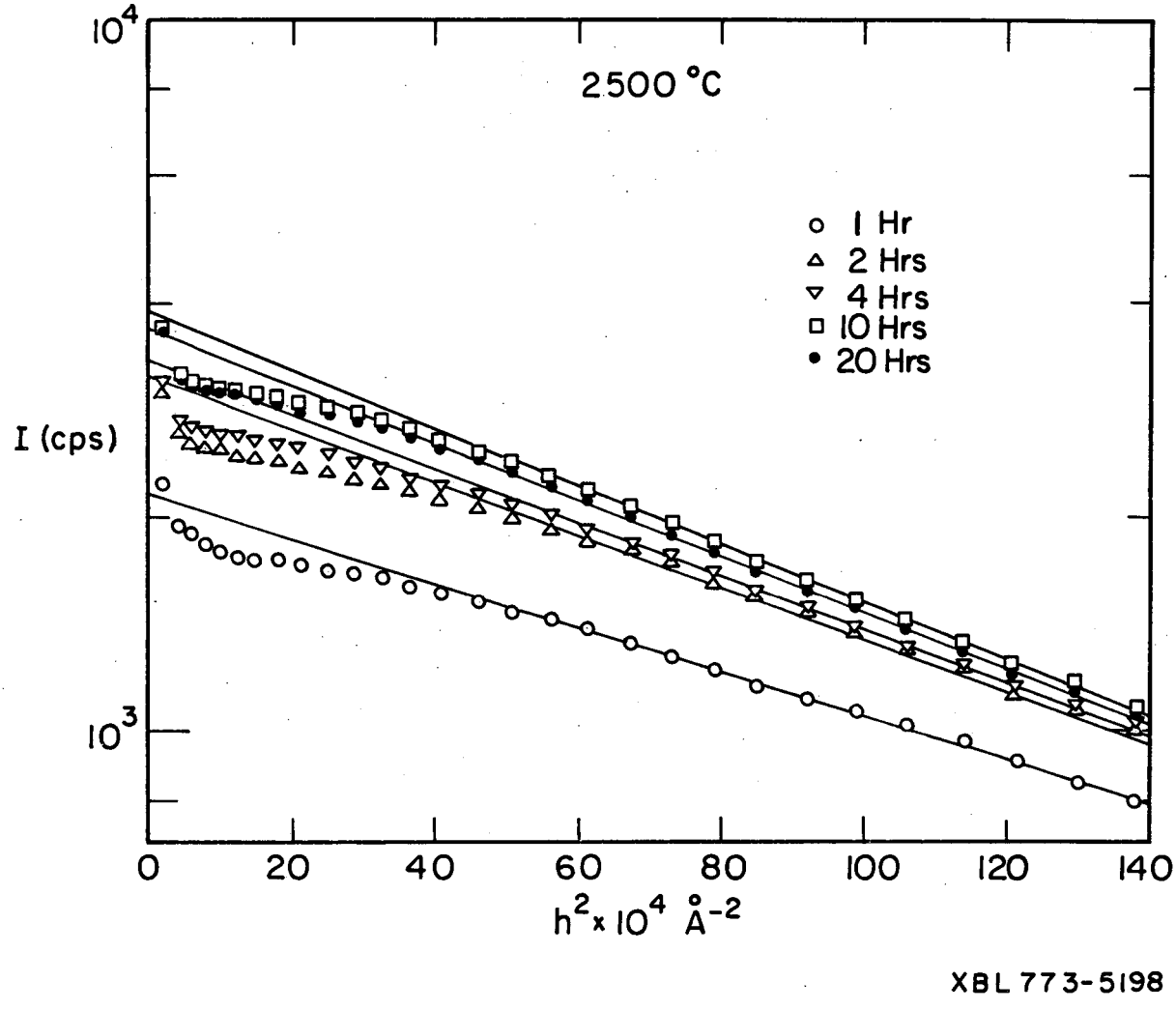
2500 °C
1 Hr
2 Hrs
4 Hrs
10 Hrs
20 Hrs
I (cps)
10^4
10^3
0
20
40
60
80
100
120
140
$h^2 \times 10^4$ Å^{-2}
XBL 773-5198

Fig. 4

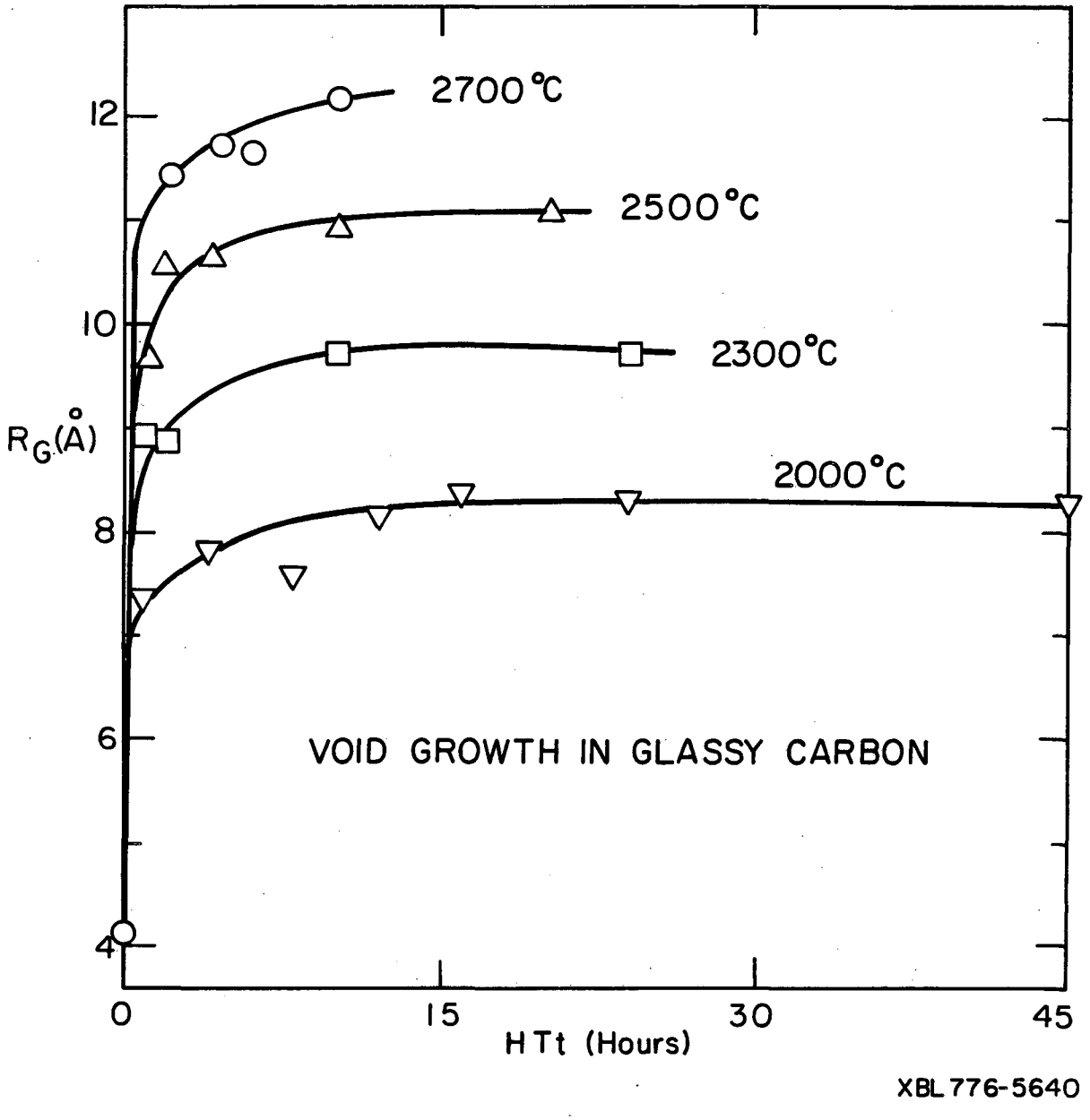
2700°C
2500°C
2300°C
2000°C
12
10
8
6
4
R_G(Å)
0
15
30
45
HTt (Hours)
VOID GROWTH IN GLASSY CARBON
XBL776-5640

Fig. 5

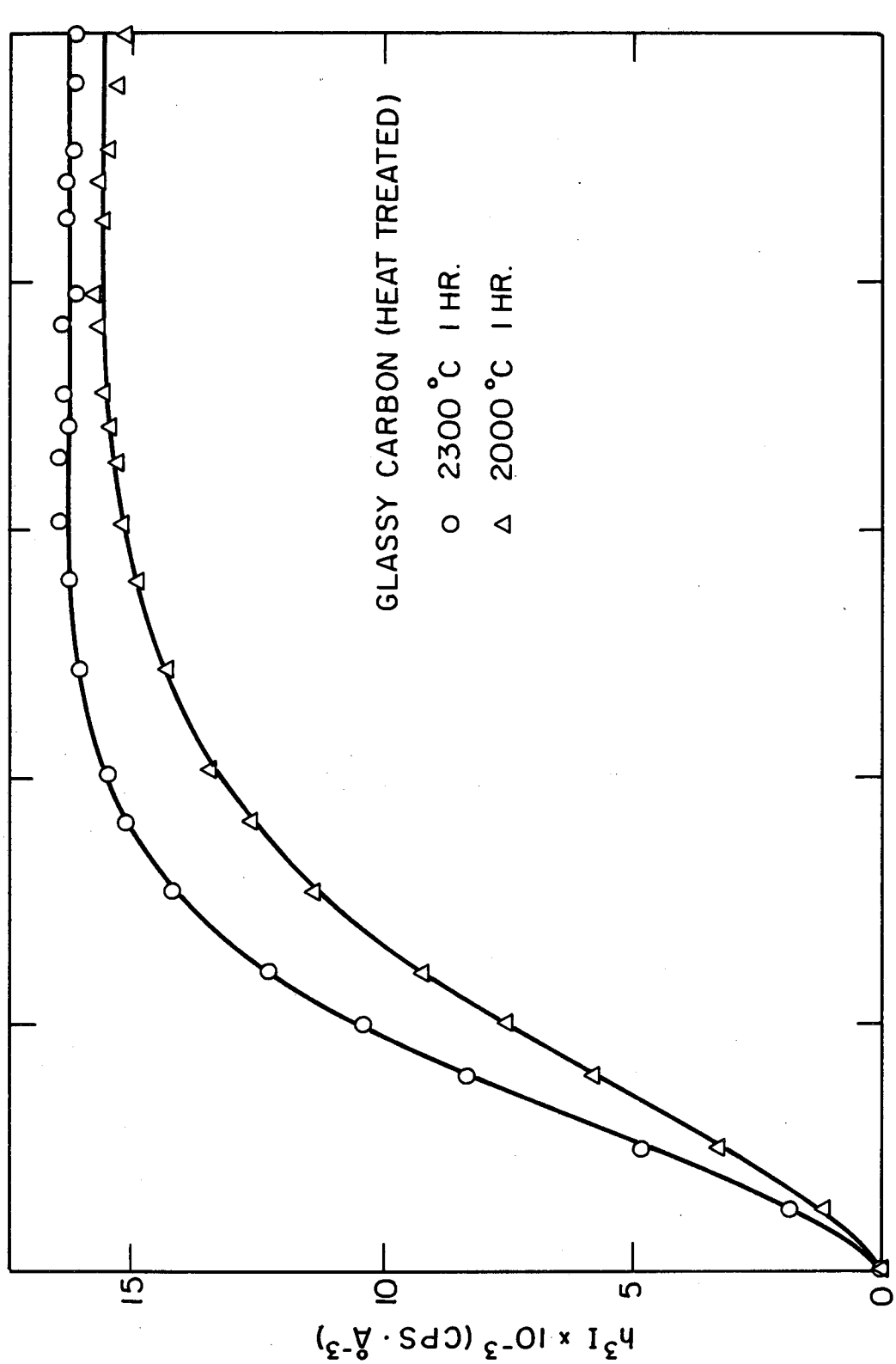

XBL781-4529

Fig. 6

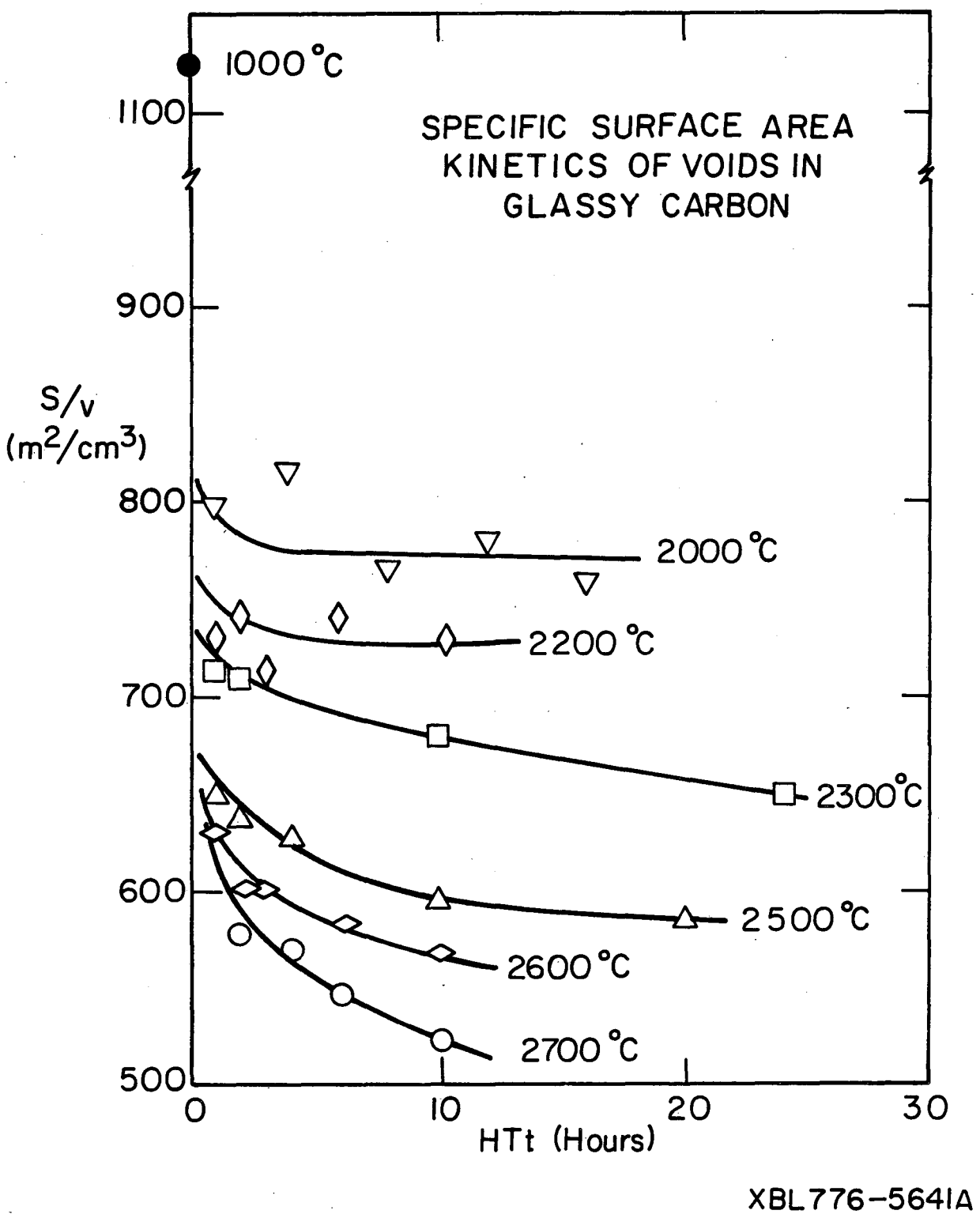
1000°C
1100
SPECIFIC SURFACE AREA
KINETICS OF VOIDS IN
GLASSY CARBON
900
S/v
(m²/cm³)
800
2000°C
2200°C
700
2300°C
600
2500°C
2600°C
2700°C
500
0
10
20
30
HTt (Hours)
XBL776-5641A

Fig. 7

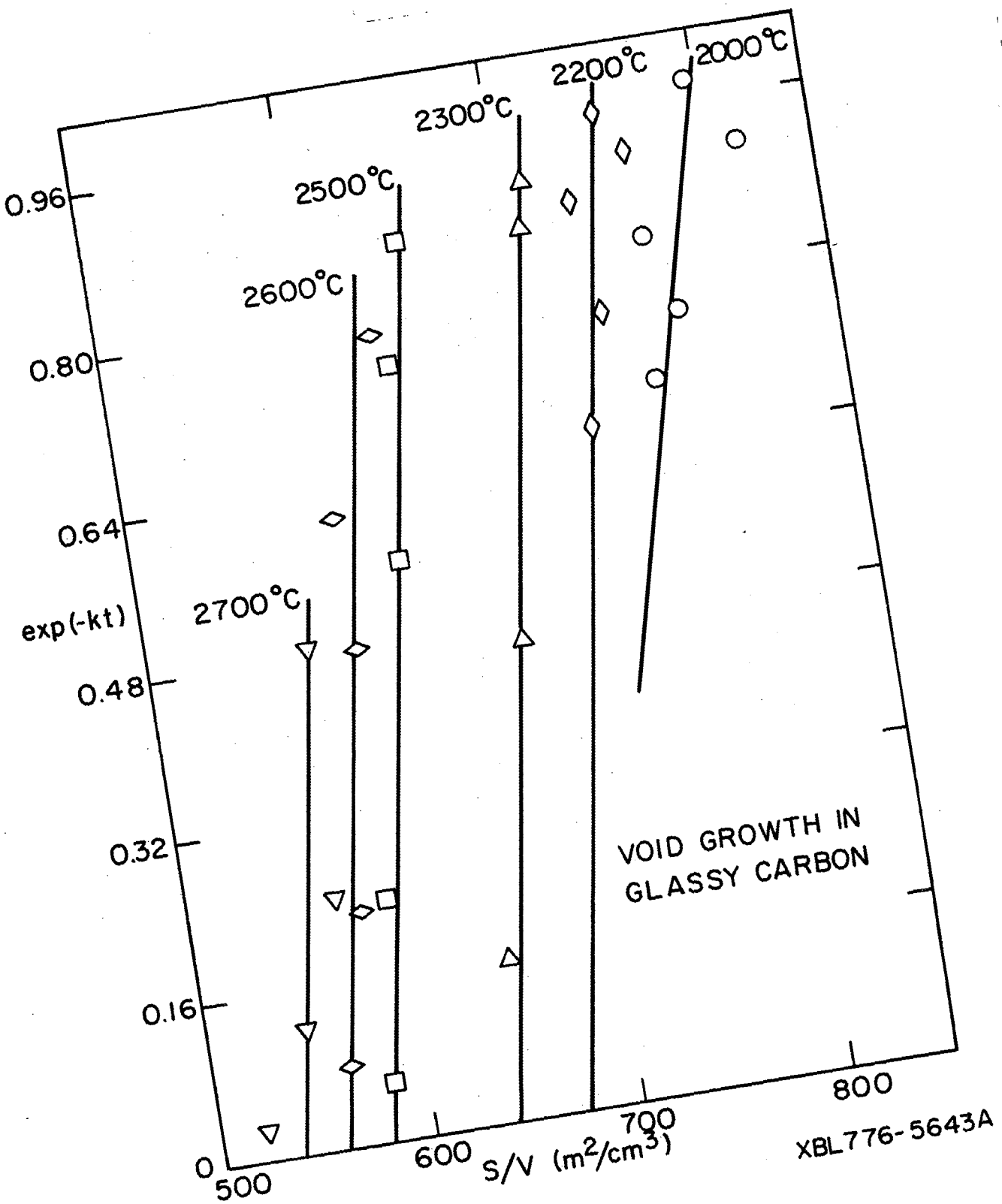
2000°C
2200°C
2300°C
2500°C
2600°C
2700°C
0.96
0.80
0.64
0.48
0.32
0.16
0
exp(-kt)
VOID GROWTH IN
GLASSY CARBON
500
600
700
800
S/V (m²/cm³)
XBL776-5643A

Fig. 8

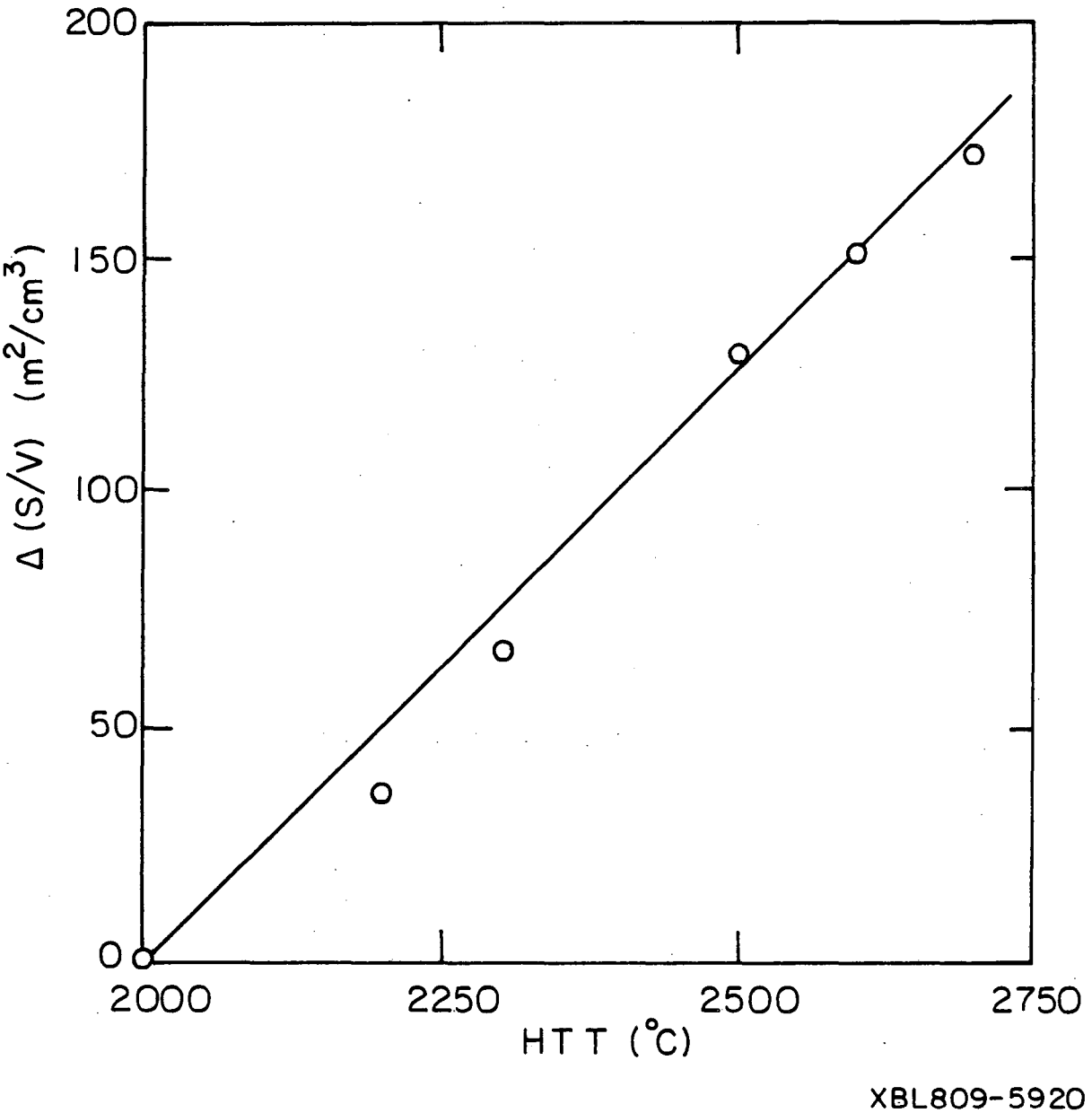
200
150
100
50
0
Δ (S/V) (m²/cm³)
2000
2250
2500
2750
HTT (°C)
XBL809-5920

Fig. 9

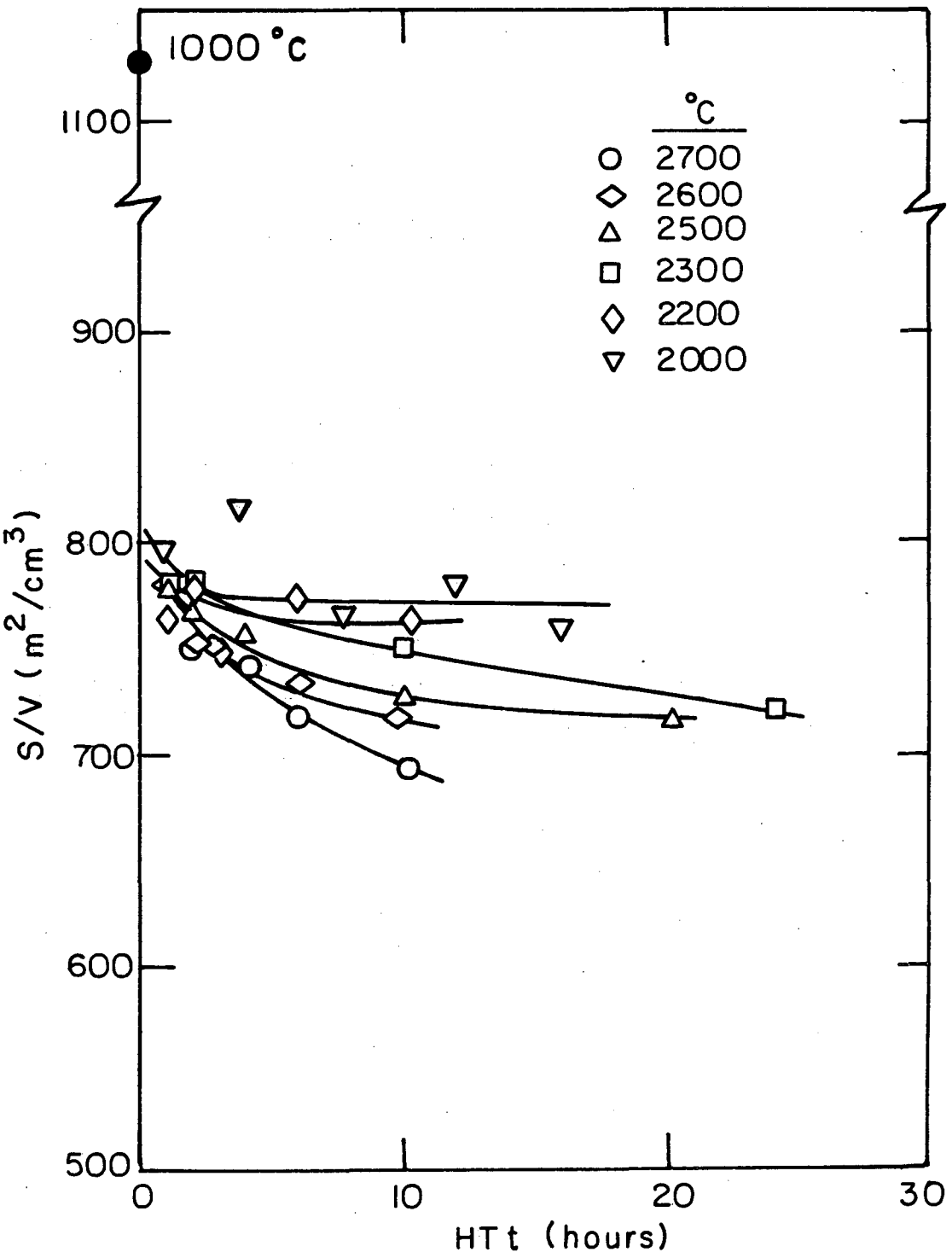

XBL809-5919

Fig. 10

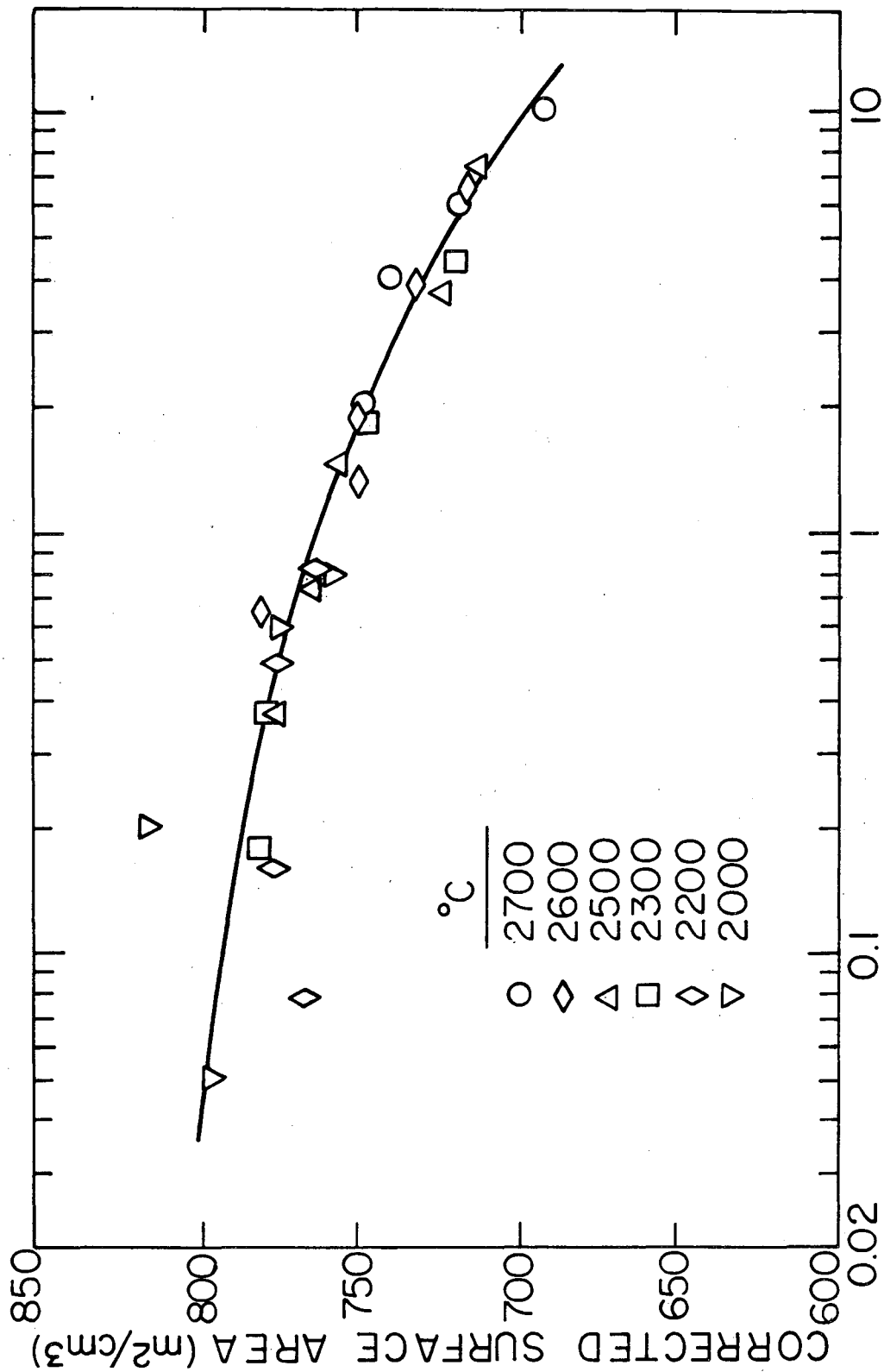

XBL809-5918

Fig. 11

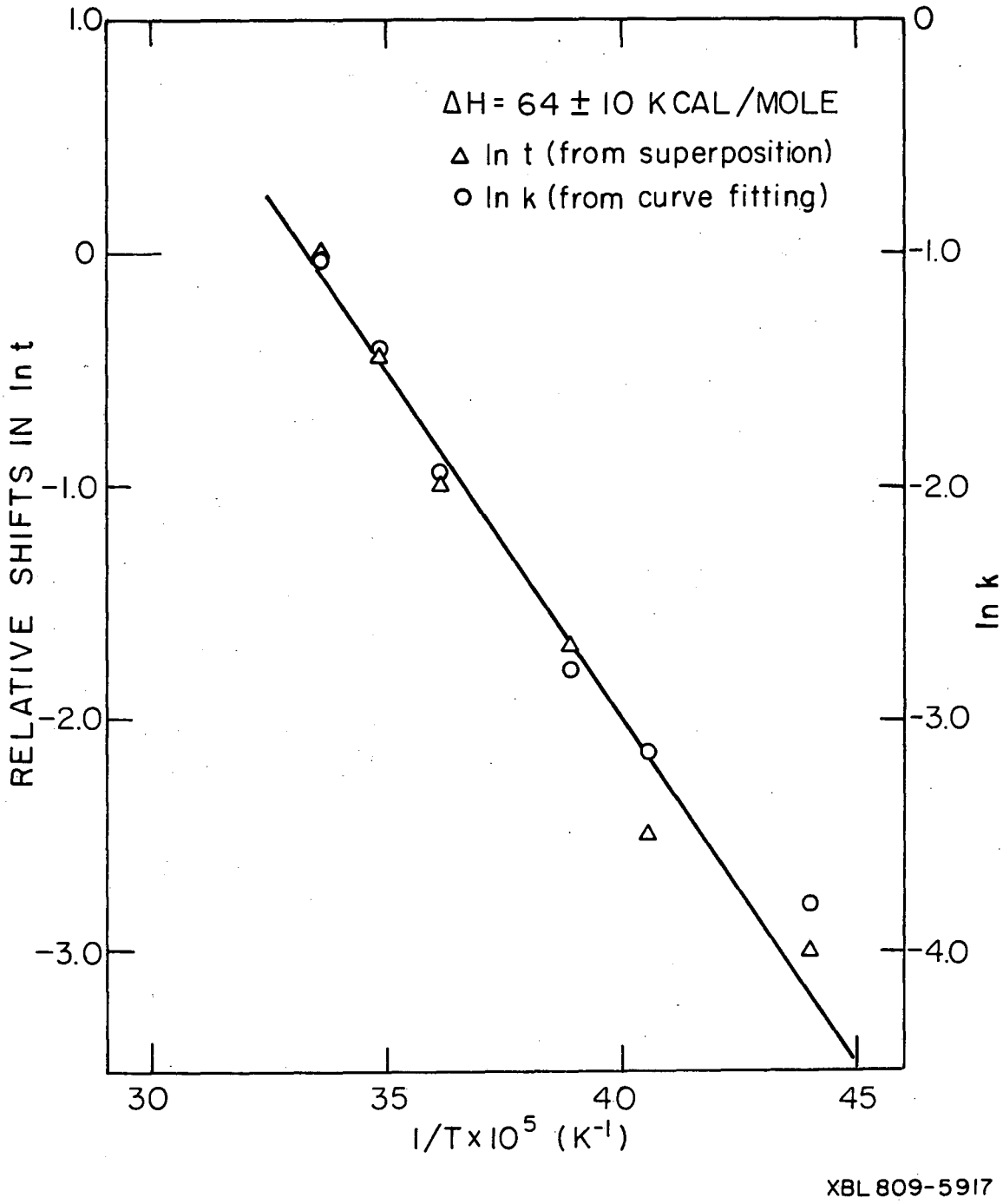
ΔH = 64 ± 10 KCAL/MOLE
Δ ln t (from superposition)
O ln k (from curve fitting)
RELATIVE SHIFTS IN ln t
ln k
1/T x 10^5 (K^-1)
1.0
0
-1.0
-2.0
-3.0
-4.0
30
35
40
45
XBL 809-5917

Fig. 12

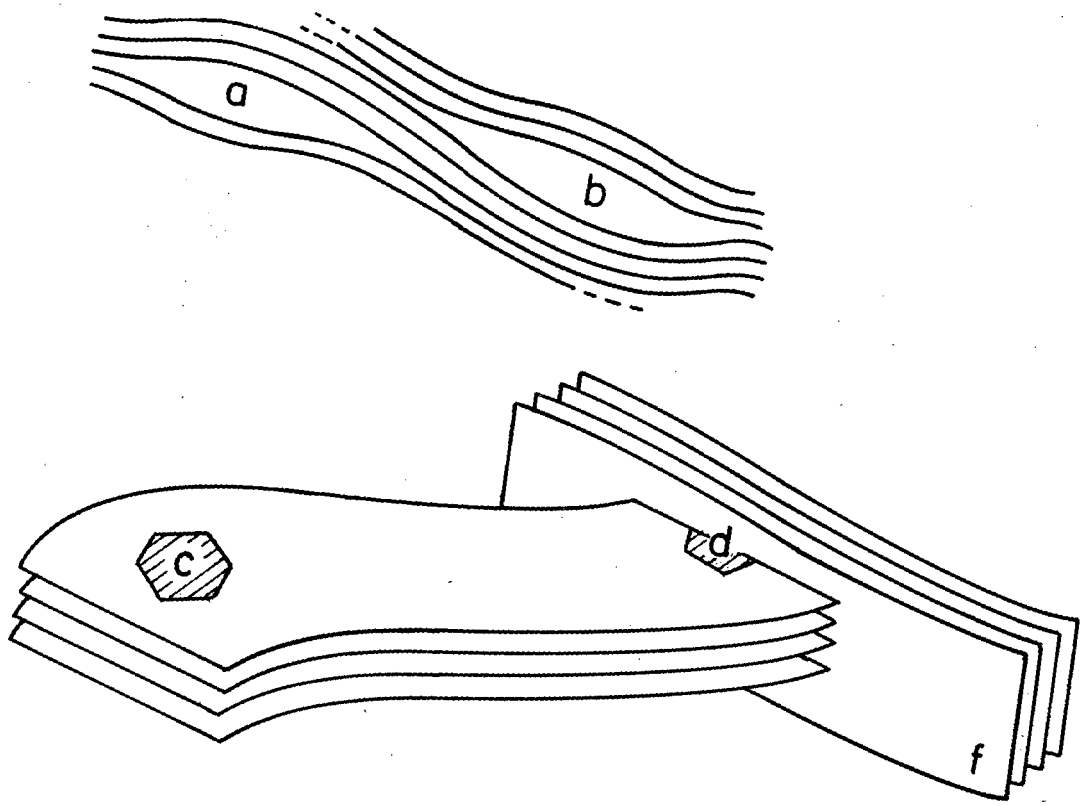

XBL 783-4760

Fig. 13

TECHNICAL INFORMATION DEPARTMENT
LAWRENCE BERKELEY LABORATORY
UNIVERSITY OF CALIFORNIA
BERKELEY, CALIFORNIA 94720